

Unraveling reaction mechanisms involving weakly bound stable nuclei

S. K. Pandit*

Nuclear Physics Division, Bhabha Atomic Research Centre, Mumbai - 400085, India

Introduction

Exploring the properties of weakly-bound stable/unstable nuclei is a topic of current interest [1–3] and also focus of the next generation of high-intensity isotope-separator on-line (ISOL) radioactive ion beam facilities. Presence of loosely bound cluster structure and exotic shapes are the distinct features seen in these nuclei with respect to the tightly-bound nuclei. Due to the low breakup threshold, population of the continuum is probable and consequently a large coupling effect is expected in the reactions involving the weakly bound nuclei at energies around the Coulomb barrier. Continuum states can be populated by direct inelastic excitation of the projectile (breakup) or nucleon transfer, leaving the ejectile in an unbound state (transfer-breakup) [1–5]. Another dominant reaction mode is transfer/capture of one of the cluster-fragment from bound/unbound state of the projectile to the target nuclei. Capture of a cluster-fragment from unbound states of the projectile can be looked upon as a two-step process, breakup followed by fusion (breakup-fusion) or incomplete fusion (ICF). This process is indistinguishable from the direct stripping of the cluster-fragment. However, it has been shown that breakup-fusion reaction is dominant over the one step stripping reaction. The admixture of these two reaction processes is generally referred to as fragment-capture [5]. Role of the breakup channels on the elastic scattering angular distribution and fusion cross-sections has been found to be significant [1–3]. The complete fusion (CF) cross section (absorption of all

the charges of the projectile) is reported to be suppressed at above-barrier energies in comparison to the predictions of the barrier penetration model [1, 6]. In case of reaction involving weakly bound nuclei with $\alpha+x$ cluster structure, e.g. ${}^6,8\text{He}$, ${}^6,7\text{Li}$, and ${}^7,9\text{Be}$, α -particle production is found to be large compared to that of the complementary fragment. Investigation of the mechanisms responsible for the large α -particle production cross sections is also a topic of current interest. Contributions to the alpha yield arising from different reaction mechanisms, such as breakup, transfer-breakup, cluster transfer, transfer followed by evaporation, incomplete fusion, compound nuclear evaporation, etc are entangled and it is not trivial to separate them from inclusive measurements. Experimentally it is challenging to disentangle these reaction processes, and exclusive measurements are essential.

To understand the experimental observables, several models based on classical, quantum mechanical, and semi-classical theory have been developed over the past years. The continuum discretized coupled channels (CDCC) method [7] provides good results concerning certain observables such as the elastic scattering, breakup, transfer-breakup and total fusion (TF) (i.e., the sum of CF and ICF) cross sections. The classical dynamical trajectory model [8] can explain the ICF and CF data simultaneously, but does not include the quantum tunneling probability. Hence in theoretical modeling, there is a strong limitation as a single model is unavailable to calculate all observables simultaneously. Further significant theoretical effort has been invested in understanding the mechanism of the large α -particle production and ICF cross sections [8–10]. Recently, using a non elastic breakup model, the cluster-stripping process

*Electronic address: sanat@barc.gov.in

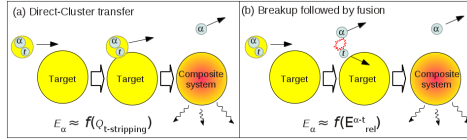


FIG. 1: Illustration of (a) direct cluster transfer and (b) breakup followed by fusion of one of the cluster fragments for a ${}^7\text{Li}(\alpha+t)$ +target reaction.

was shown to be the dominant mechanism for ICF [9]. In other studies, fusion of the breakup fragments was considered to be the main ICF mechanism [5, 8, 10, 12]. Calculations assuming both cluster stripping [9] and breakup-fusion [5, 8, 10, 12] mechanisms have successfully reproduced experimental inclusive α yields and/or fusion data to a similar extent. Further, it has also been suggested that breakup-fusion and transfer to the continuum of the target are equivalent [10]. It is therefore essential to have experimental data populating the bound states and the continuum with comparable magnitude to discriminate between the two widely different mechanisms. As depicted in Fig. 1, while the outgoing α particle has access to the reaction Q value in the case of direct stripping, the triton fusion (second step) Q value can not be shared with the α particle (produced in the first step) in the two-step breakup-fusion process. A suitable choice of experimental conditions could therefore allow a region which is exclusively populated by only one of these processes to be studied.

Experimental details

To understand the reaction mechanisms, two sets of coincident measurements have been carried out (a) exclusive measurements of breakup fragments and (b) particle- γ in coincidence. All the experiments were carried out at the BARC-TIFR Pelletron-Linac facility, Mumbai, with ${}^7\text{Li}$ beams. Measurements of breakup fragments in coincidence were performed at 24, 28 and 30 MeV for ${}^7\text{Li}+{}^{89}\text{Y}$, ${}^{93}\text{Nb}$ systems. Self-supporting ${}^{89}\text{Y}$ and ${}^{93}\text{Nb}$ foils of thicknesses ~ 2 mg/cm² and ~ 1.7 mg/cm² were used as a target. In addition to

the particle- γ coincidence measurements performed at 24 and 28 MeV for ${}^7\text{Li}+{}^{93}\text{Nb}$ system, residues formed due to complete fusion and fragments capture, and the target like nuclei followed by nucleon transfer reactions were also measured by in-beam and off-beam singles γ -ray counting methods.

In case of measurements of breakup and transfer-breakup reactions, the requirements of high granularity to detect low-lying resonant states and large solid angle to measure low cross section events were achieved using segmented large area Si-telescopes of active area 5×5 cm². The ΔE detector (50 μm thick) was single-sided and the E detector (1.5 mm thick) was double-sided with 16 strips allowing a maximum of 256 pixels. Two such telescopes, set 30° apart, were mounted at a distance of 16 cm from the target on a movable arm in a scattering chamber. In this geometry, the cone angle between the two detected fragments ranged from 1° to 24°. The angular range 30°-130° (around the grazing angle) was covered by measurements at different angle settings. Three Si surface-barrier detector telescopes (thicknesses: $\Delta E \sim 20$ -50 μm , $E \sim 450$ -1000 μm) were used to obtain the elastic scattering angular distribution at forward angles (25°-40°) where the count rate is too high for the strip detectors to cope with. Two Si surface-barrier detectors (thickness ~ 300 μm) were kept at $\pm 20^\circ$ for absolute normalization. The detectors were calibrated using the known α energies from a ${}^{239}\text{Pu}$ - ${}^{241}\text{Am}$ -source and the ${}^7\text{Li} + {}^{12}\text{C}$ reaction at 24 MeV.

In the exclusive measurement of prompt γ -ray and α -particle, prompt γ -ray transitions were detected using the Indian National Gamma Array (INGA), consisting of 18 Compton suppressed high purity germanium (HPGe) clover detectors [15]. Three Si surface barrier telescopes (thicknesses $\Delta E \sim 15$ -30 μm , $E \sim 300$ -5000 μm) were kept at 35°, 45° and 70° for the detection of α particles around the grazing angle. One Si surface barrier detector (thickness ~ 300 μm) was fixed at 20° to monitor Rutherford scattering for absolute normalization purposes. The time stamped data were collected using a digital